Demonstration of a compact temperature sensor based on first-order Bragg grating in a tapered fiber probe

Jun-long Kou,[1] Sun-jie Qiu,[1] Fei Xu,[1,*] and Yan-qing Lu[1,2]

[1]*College of Engineering and Applied Sciences and National Laboratory of Solid State Microstructures, Nanjing University, Nanjing 210093, China*

[2]*yqlu@nju.edu.cn*

**feixu@nju.edu.cn*

Abstract: We experimentally demonstrate an all-silica first-order fiber Bragg grating (FBG) for high temperature sensing by focused ion beam (FIB) machining in a fiber probe tapered to a point. This 61-period FBG is compact (~36.6 μm long and ~6.5 μm in diameter) with 200-nm-deep shallow grooves. We have tested the sensor from room temperature to around 500 °C and it shows a temperature sensitivity of nearly 20 pm/°C near the resonant wavelength of 1550 nm. This kind of sensor takes up little space because of its unique geometry and small size and may be integrated in devices that work in harsh environment or for detecting small objects.

OCIS codes: (060.2370) Fiber optics sensors; (120.6780) Temperature.

References and links

1. Y. P. Wang, "Review of long period fiber gratings written by CO_2 laser," J. Appl. Phys. **108**(8), 081101 (2010).
2. Y.-J. Rao, Y.-P. Wang, Z. L. Ran, and T. Zhu, "Novel fiber-optic sensors based on long-period fiber gratings written by high-frequency CO_2 laser pulses," J. Lightwave Technol. **21**(5), 1320–1327 (2003).
3. Y. Kondo, K. Nouchi, T. Mitsuyu, M. Watanabe, P. G. Kazansky, and K. Hirao, "Fabrication of long-period fiber gratings by focused irradiation of infrared femtosecond laser pulses," Opt. Lett. **24**(10), 646–648 (1999).
4. L. B. Fu, G. D. Marshall, J. A. Bolger, P. Steinvurzel, E. C. Magi, M. J. Withford, and B. J. Eggleton, "Femtosecond laser writing Bragg gratings in pure silica photonic crystal fibres," Electron. Lett. **41**(11), 638–640 (2005).
5. C. Y. Lin and L. A. Wang, "A wavelength- and loss-tunable band-rejection filter based on corrugated long-period fiber grating," IEEE Photon. Technol. Lett. **13**(4), 332–334 (2001).
6. T. L. Lowder, K. H. Smith, B. L. Ipson, A. R. Hawkins, R. H. Selfridge, and S. M. Schultz, "High-temperature sensing using surface relief fiber Bragg gratings," IEEE Photon. Technol. Lett. **17**(9), 1926–1928 (2005).
7. G. Brambilla, V. Pruneri, L. Reekie, C. Contardi, D. Milanese, and M. Ferraris, "Bragg gratings in ternary SiO_2:SnO_2:Na_2O optical glass fibers," Opt. Lett. **25**(16), 1153–1155 (2000).
8. F. Xu, G. Brambilla, J. Feng, and Y.-Q. Lu, "A microfiber Bragg grating based on a microstructured rod: a proposal," IEEE Photon. Technol. Lett. **22**(4), 218–220 (2010).
9. J.-l. Kou, Z.-d. Huang, G. Zhu, F. Xu, and Y.-q. Lu, "Wave guiding properties and sensitivity of D-shaped optical fiber microwire devices," Appl. Phys. B **102**(3), 615–619 (2011).
10. H. Xuan, W. Jin, and M. Zhang, "CO_2 laser induced long period gratings in optical microfibers," Opt. Express **17**(24), 21882–21890 (2009).
11. H. Xuan, W. Jin, and S. Liu, "Long-period gratings in wavelength-scale microfibers," Opt. Lett. **35**(1), 85–87 (2010).
12. A. Martinez, I. Y. Khrushchev, and I. Bennion, "Thermal properties of fibre Bragg gratings inscribed point-by-point by infrared femtosecond laser," Electron. Lett. **41**(4), 176–178 (2005).
13. J. L. Kou, J. Feng, Q. J. Wang, F. Xu, and Y. Q. Lu, "Microfiber-probe-based ultrasmall interferometric sensor," Opt. Lett. **35**(13), 2308–2310 (2010).
14. J. L. Kou, J. Feng, L. Ye, F. Xu, and Y. Q. Lu, "Miniaturized fiber taper reflective interferometer for high temperature measurement," Opt. Express **18**(13), 14245–14250 (2010).
15. F. Renna, D. Cox, and G. Brambilla, "Efficient sub-wavelength light confinement using surface plasmon polaritons in tapered fibers," Opt. Express **17**(9), 7658–7663 (2009).
16. W. Streifer, D. Scifres, and R. Burnham, "Coupling coefficients for distributed feedback single- and double-heterostructure diode lasers," IEEE J. Quantum Electron. **11**(11), 867–873 (1975).

#150910 - $15.00 USD Received 12 Jul 2011; revised 7 Aug 2011; accepted 22 Aug 2011; published 6 Sep 2011

17. W. Streifer and A. Hardy, "Analysis of two-dimensional waveguides with misaligned or curved gratings," IEEE J. Quantum Electron. **14**(12), 935–943 (1978).
18. M. L. Åslund, J. Canning, M. Stevenson, and K. Cook, "Thermal stabilization of Type I fiber Bragg gratings for operation up to 600 ° C," Opt. Lett. **35**(4), 586–588 (2010).
19. H. Y. Choi, K. S. Park, S. J. Park, U. C. Paek, B. H. Lee, and E. S. Choi, "Miniature fiber-optic high temperature sensor based on a hybrid structured Fabry-Perot interferometer," Opt. Lett. **33**(21), 2455–2457 (2008).
20. S. Ju, P. R. Watekar, and W.-T. Han, "Enhanced sensitivity of the FBG temperature sensor based on the PbO-GeO_2-SiO_2 glass optical fiber," J. Lightwave Technol. **28**(18), 2697–2700 (2010).
21. J. Wang, B. Dong, E. Lally, J. Gong, M. Han, and A. Wang, "Multiplexed high temperature sensing with sapphire fiber air gap-based extrinsic Fabry-Perot interferometers," Opt. Lett. **35**(5), 619–621 (2010).

1. Introduction

Over the last two decades, optical sensors based on fiber gratings, including fiber Bragg gratings (FBGs) and long-period gratings (LPGs), have attracted much attention due to their widespread applications in various physical or chemical parameter measurements such as refractive index, strain and temperature. Standard fiber gratings fabricated by exposing photosensitive fibers to an intense ultraviolet interference pattern can be normally used for measuring relatively low temperature below 200 °C. Various fabrication methods such as CO_2 laser irradiation [1,2], femtosecond laser exposure [3,4] and etched corrugations [5,6], have been demonstrated to write gratings for high temperature sensing in different types of optical fibers [7]. However, these gratings fabricated in thick fibers have weak index modulation and the grating lengths are at least several millimeters, which greatly limit the size of sensor heads. One alternative solution is to write short and strong grating in a micrometer-order-diameter microfiber. Several kinds of techniques on fabrication microfiber gratings have been proposed, for example, wrapping a microfiber on a microstructured rod [8,9], using CO_2 lasers [10] and femtosecond lasers [11,12]. The former can be used to realize compact FBG but it needs extra polymer coating which is not suitable for high temperature sensing. The latter can only be used to write LPG or long high-order FBG which means that the grating length is still long.

In this letter, we experimentally demonstrate a compact all-silica deeply-corrugated first-order-FBG for high-temperature sensing by focused ion beam (FIB) machining in a tapered non-photosensitive single-mode-fiber probe with a sharp profile. FIB technology is perfect for micro-machining and nano-fabrication due to its small and controllable spot size and high beam current density. It has been successfully used to directly micromachine micro-cavities [13,14] or to modify the tip geometry in a subwavelength fiber [15]. Here, we directly carve periodic grooves on a sharp micrometer scale tapered fiber probe (TFP), which is around 6.5 μm in diameter. The groove period is 600 nm for the first order resonance. The groove depth is 0.2 μm and the total grating length is 36.6 μm. The all-silica TFP grating (TFPG) has a temperature sensitivity of ~20 pm/°C with a reflection peak-to-trough ratio of > 10 dB. Its extremely small size, all fiber connection, high sensitivity and especially unique structure offer possible potentials for fast-response high temperature sensing, particularly in small object, *e.g.* bubbles.

2. Fabrication of the TFPG

A commercial pipette puller (model P2000) is utilized to fabricate the TFPG [15]. In order to get a sharp and smooth taper profile, we have optimized the CO_2 laser power and pulling velocity. The manufactured TFPG has a long pigtail to allow prompt link to other optical fiber components. The tip is first coated with a thin layer of aluminum (Al) by magnetron sputtering. The Al layer is used as a conductive layer to prevent gallium ion accumulation in the FIB micromachining process. Then, the Al-coated fiber tip is fixed stably in the FIB machining chamber (Strata FIB 201) using a copper tape. We use a gallium ion beam perpendicular to the fiber axis. The shape of the beam is cylindrical symmetric with a diameter of about 20 nm. With such accuracy, groove length can be controlled precisely. In our experiment, the grating is made through a two-step process where the second step under the same beam current is used to improve the surface smoothness. Finally, the TFP is immersed in hydrochloric acid for about 20

#150910 - $15.00 USD Received 12 Jul 2011; revised 7 Aug 2011; accepted 22 Aug 2011; published 6 Sep 2011

minutes to totally remove the Al layer before it is cleaned with deionized water. Figure 1 shows the FIB picture of the periodic structures from the side view. The grating has shallow corrugations of period Λ = 600 nm with 61 periods. The total length is about 36.6 μm, which is extremely short. The groove face is very sharp and smooth. Every groove is 200 nm in depth, located at the position with the local radius around r = 3.25 μm.

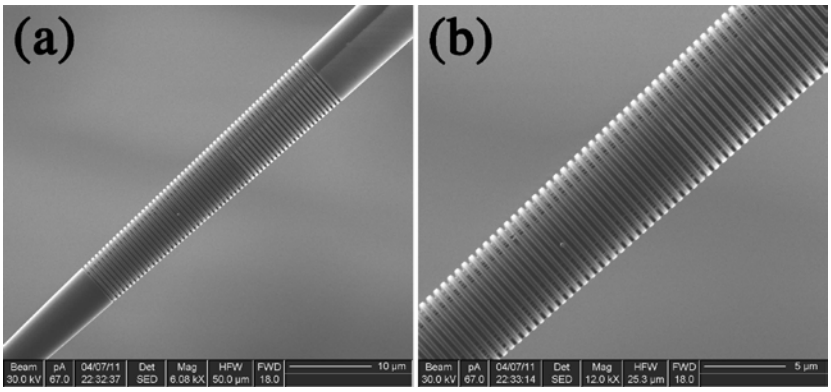

Fig. 1. (a) FIB picture of the TFPG with 61 periods (~36.6 μm in length and Λ = 600 nm). (b) Magnified picture of the grating.

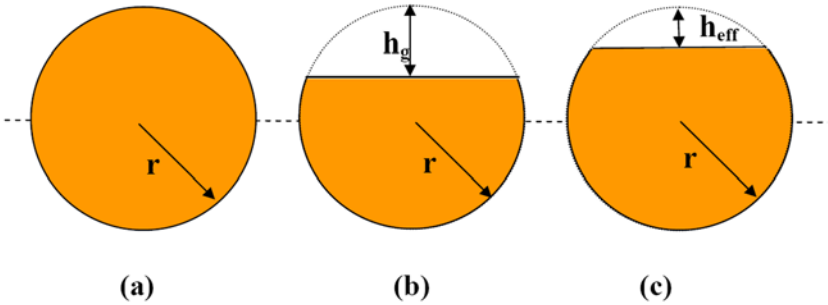

Fig. 2. The cross-sections of (a) an un-etched fiber, (b) an etched fiber and (c) an equivalent unperturbed geometry, respectively. h_g is the groove height and h_{eff} is effective height.

As in a planar corrugated Bragg grating, the Bragg wavelength of the grating is expressed by $\lambda_B = 2n_{eff}\Lambda$, where n_{eff} is the mode effective refractive index in the equivalent unperturbed geometry, and Λ is the period. The mode field and n_{eff} in the equivalent unperturbed waveguide geometry can be derived from the perturbed (straight) geometry using the method developed by W. Streifer [16,17]. Figure 2 shows the cross-sections of an un-etched fiber, an etched fiber and the equivalent unperturbed geometry with this method, which shifts the boundary between air and silica to compensate for the different geometry [16,17], respectively. The effective groove height h_{eff} of the equivalent unperturbed geometry satisfies:

$$\begin{cases} (1-\tau)(\theta_g - \sin\theta_g \cos\theta_g) = \theta_{eff} - \sin\theta_{eff}\cos\theta_{eff} \\ \theta_g = \arccos\{(r-h_g)/r\} \\ \theta_{eff} = \arccos\{(r-h_{eff})/r\} \end{cases} \quad (1)$$

where τ is the grating duty cycle, h_g is the groove height and r is the fiber radius, respectively. In our device, r = 3.25 μm, τ = 0.5 and h_g = 0.2 μm. We find h_{eff} = 0.125 μm by solving Eq. (1) and n_{eff} = 1.433 by utilizing a finite element analysis. Thus, the Bragg wavelength is 1720 nm for the

#150910 - $15.00 USD Received 12 Jul 2011; revised 7 Aug 2011; accepted 22 Aug 2011; published 6 Sep 2011

fundamental mode. It is different with the following experimental results (~1550 nm). The possible reason is that higher order mode is excited in the multi-mode fiber taper because the higher order mode has more overlap with the side corrugated surface. Moreover, the grating is nearly liner chirped because the taper is nonuniform. It agrees well with the following experimental results. The chirp can be cancelled if we use uniform tapered fiber.

3. Experiments and discussions

The reflection of the TFPG in Fig. 1 is measured with a broadband source near 1550 nm and an Ando AQ6317B optical spectrum analyzer (OSA) through a circulator, the same setup as in [13]. Same as our previous experiment, before micromachining the tapered fiber probe; it displays an ignorable reflection of less than −100 dB over the whole broadband spectrum. Hence, the reflection at the tip end is negligible and the detected signal only results from the light reflected by the grating.

For most of these applications the required operational temperature only needs to be as high as 400 °C [18]. So we characterize the thermal response of the TFPG from room temperature (21 °C) to 440 °C which can meet conventional applications. The TFPG is heated up in a micro-furnace and the temperature is measured by a thermocouple (TES-1310, Type K, TES Electrical Electronic Corp.). The spectrum and temperature are recorded when both of them are stable for several minutes.

We have to point out that 440 °C is not the temperature measurement limitation of the grating sensor. In [6], a geometric-modulated or surface-relief grating on a d-shaped silica fiber works up to > 1000 °C. Our grating has the same work mechanism with [6] and is also a physical change in the geometry. It can work before the geometry is destroyed. The limitation of the temperature measurement should be much higher than 440 oC. Furthermore, in our previous work about a fiber tip temperature sensor based on FIB-machined micro-cavity, we have measured the temperature up to ~550 °C [14].

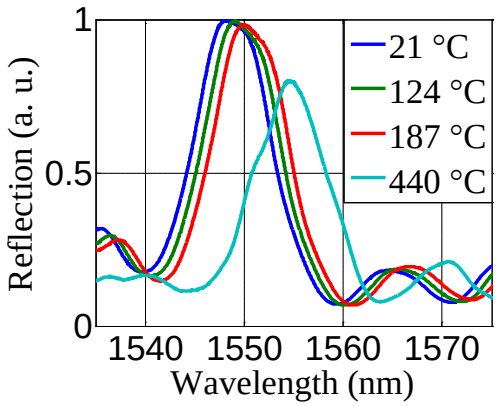

Fig. 3. Reflection spectra of the TFPG in air at different temperatures.

The resonant spectra of the TFPG at different temperatures (21 °C, 124 °C, 187 °C and 440°C) are shown in Fig. 3. The Bragg wavelength is ~1550 nm, with excited higher order mode as deduced from our theoretical calculation. The spectra indicate an extinction ratio of ~11 dB at the Bragg wavelength which is achieved with a 36.6 μm long Bragg grating and is similar with or even better than some other long length fiber gratings, enough for sensing applications.

The temperature sensitivity S_T is defined as the resonant wavelength shift divided by the corresponding temperature change. S_T depends on temperature through the thermo-optics and/or thermal expansion effect [19]:

#150910 - $15.00 USD Received 12 Jul 2011; revised 7 Aug 2011; accepted 22 Aug 2011; published 6 Sep 2011

$$S_T = \frac{d\lambda_r}{dT} = 2\left(\sigma_T \Lambda \frac{\partial n_{eff}}{\partial n_{silica}} + r\Lambda\alpha_T \frac{\partial n_{eff}}{\partial r} + \Lambda\alpha_T n_{eff}\right) \quad (2)$$

where σ_T (1.4×10^{-5} /°C) is the thermo-optics coefficient and α_T (5.5×10^{-7} /°C) is the thermal expansion coefficient. Temperature change influences three items: temperature-induced index variation, taper volume variation and temperature-induced grating length variation. According to our calculations, thermal expansion effect [the second and third part of Eq. (2)] contributes little to the total sensitivity (< 6%), mainly due to the low thermal expansion coefficient of silica. The first one is about 15 ~25 pm/°C and dominates in temperature sensing. Moreover, in the first part of Eq. (2), $\partial n_{eff} / \partial n_{silica}$ is nearly 1 and does not change much with the microfiber diameter, which means that the most efficient method to increase temperature sensitivity is to use fiber with higher thermo-optics coefficient.

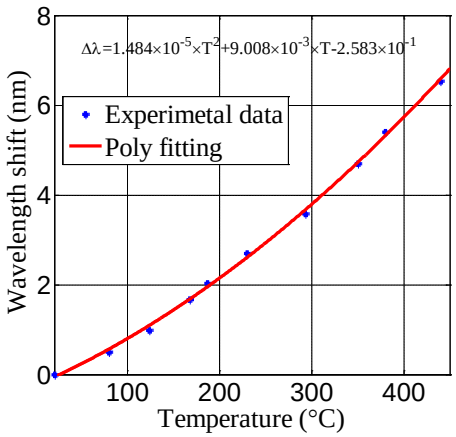

Fig. 4. Dependence of the measured wavelength shift on temperature. The asterisk represents the measured results while the solid line is the linear fitting result.

Figure 4 displays the measured resonant wavelength shifts (Δλ) on temperature (T). As the temperature increases, the resonant wavelength shifts to longer wavelength. A poly fitting is used across the entire calibration range. The average sensitivity of the device is ~20 pm/°C, which is very close to the theoretical result, higher than or similar with previous fiber grating sensors. Higher sensitivity can be obtained by optimizing the profile of the TFPG or use special fiber taper with higher thermo-optics coefficient.

The resolution of a sensor is limited by several practical terms, *e.g.* the width of reflection peak, detection method, spectral variation and intrinsic sensor noise. For our devices, the bandwidth of the reflection peak (several nm) and the OSA resolution are the main issues. The reflection peak bandwidth can be narrowed by fabricating the grating with more periods in a more uniform taper region. On the other hand, we can use a power meter accompanied by a tunable laser with higher resolution which will give a more precise peak value.

The reproducibility and stability of a geometric-modulated grating depend on the geometric stability. The experimental results in [6] show a good reproducibility and stability by heating and cooling it between room temperature to 1000 °C. Our grating has the same working mechanism thus it can be stable and keep good reproducibility before the material melts and the structure is destroyed.

4. Discussions and Conclusions

Conventional FBG is fabricated by writing variation of refractive index into the core of Ge-doped silica fiber using UV light by phase mask. The index modulation is very weak and is

#150910 - $15.00 USD Received 12 Jul 2011; revised 7 Aug 2011; accepted 22 Aug 2011; published 6 Sep 2011

unstable when temperature is high. Compared with the standard FBG grating, the main advantages of our proposed grating are the compact size, stable geometric modulation, and flexible fabrication technique without the limitation of fiber material.

First, the standard FBG is usually up to centimeters in length [20] which is much longer than our FIB-milled one. Device with long length is usually much difficult to handle and move in air or fluid and it is often easy to be influenced by other effect, *e.g.*, bending, strain and vibration. However, our FIB-milled FBG in a tapered fiber tip is much compact (~36.6 μm long located in ~6.5 μm in diameter) which may be useful in detecting ultra-tiny object, *e.g.* bubbles.

Second, the common FBG fabricated by UV light usually cannot serve in environment with temperature above 200 °C, because the index modulation will degrade after long-time exposure in high temperature environment. However, FIB-machined grating is different because the index modulation results from the corrugations on the fiber tip surface. It means that the grating can be very stable if the fiber material (silica) does not melt and the corrugations will not be destroyed.

Third, we emphasize on the method (*i.e.* FIB) of fabricating the grating. The FIB milling can be extended to micromachining fibers made of different materials such as sapphire whose melting point can be well above 2000 °C [21], which means that it is possible to realize an ultra-high temperature sensor.

In summary, we experimentally demonstrate an all-silica FBG for high-temperature sensing by FIB machining in a tapered fiber probe with a sharp profile. The grating is relatively short (only 36.6 μm) with shallow corrugations in a fiber taper with diameter around 6.5 μm. The calibration of the sensor is carried out from room temperature to around 500 °C and shows a temperature sensitivity of ~20 pm/°C. The resonance at the Bragg wavelength is achieved with as few as 61-period and 200-nm-deep corrugations on the taper surface. All these performance are better than or similar with other fiber gratings with much bigger size or length. Its advantages of compact size, high sensitivity, easy interrogation, simple fabrication and unique geometry offer great possible prospects for developing novel high temperature sensors for small space.

Acknowledgments

This work is supported by National 973 program under contract No. 2010CB327803, 2012CB921803 and 2011CBA00200, NSFC program No. 11074117 and 60977039. The authors also acknowledge the support from the Priority Academic Program Development of Jiangsu (PAPD) and the Fundamental Research Funds for the Central Universities.

#150910 - $15.00 USD Received 12 Jul 2011; revised 7 Aug 2011; accepted 22 Aug 2011; published 6 Sep 2011